CrossMark

ORIGINAL ARTICLE

Non-random spatial relationships between mast cells and microvessels in human endometrial carcinoma

Diego Guidolin[1] · Christian Marinaccio[2] · Cinzia Tortorella[1] · Tiziana Annese[2] · Simona Ruggieri[2] · Nicoletta Finato[3] · Enrico Crivellato[4] · Domenico Ribatti[2,5]

Abstract Mast cells (MCs) accumulate in the stroma surrounding tumors, where they secrete angiogenic cytokines and proteases, and an increased number of MCs have been demonstrated in angiogenesis associated with solid and hematological tumors. The aim of this study is to contribute to the knowledge of distribution of MCs in tumors, investigating the pattern of distribution of tryptase-positive MCs around the blood vessels in human endometrial carcinoma samples by introducing a quantitative approach to characterize their spatial distribution. The results have shown that in human endometrial cancer bioptic specimens the spatial distribution of MCs shows significant deviation from randomness as compared with control group in which, instead, the spatial distribution of MCs is consistent with a random distribution. These findings confirm that MCs enhance tumor angiogenesis and their preferential localization along blood vessels and sites of new vessel formation sustaining the suggestion for an association between MCs and angiogenesis. However, this spatial association between vessels and MCs might simply reflect migrating MCs from the blood stream at vessel growing sites.

Keywords Endometrial carcinoma · Mast cell · Spatial distribution · Tumor growth

✉ Domenico Ribatti
ribatti@anatomia.uniba.it; domenico.ribatti@uniba.it

1   Department of Molecular Medicine, University of Padova Medical School, Padua, Italy

2   Department of Basic Medical Sciences, Neurosciences, and Sensory Organs, University of Bari Medical School, Piazza Giulio Cesare, 11, 70124 Bari, Italy

3   Department of Biological and Medical Sciences, University of Udine Medical School, Udine, Italy

4   Department of Experimental and Clinical Medical Sciences, University of Udine Medical School, Udine, Italy

5   National Cancer Institute "Giovanni Paolo II", Bari, Italy

Introduction

The concept that cancer and inflammation are linked was suggested as far back at the nineteenth century by Rudolf Virchow, who was the first to establish a causative connection between the inflammatory infiltrate and cancer.

Mast cells (MCs) accumulate in the stroma surrounding tumors, where they secrete angiogenic cytokines and proteases. We have previously demonstrated that in human endometrial carcinoma angiogenesis is highly correlated with tryptase-positive MC cell counts and that these parameters parallel with tumor progression [1]. We have further correlated in the same tumor specimens and the number of CD8-positive T cells, and we have shown that both counts correlate and increase in parallel with tumor progression [2].

The spatial distribution of MCs inside the tumor stroma of different tumors has been poorly investigated. We have previously studied the pattern of distribution of MCs in biopsy samples from four different human solid tumors, including endometrial adenocarcinoma, primary melanoma, non-small cell lung carcinoma, and cutaneous melanoma [3]. The results have shown that the spatial distribution of MCs was virtually random and was very similar in all the tumor types, and independent from the selected area of the lesion (marginal or central area), and suggested that MC–MC interactions could play a minor role in the formation of the MC pattern in neoplastic tissue.

Springer

The aim of this study was to further contribute to the knowledge of tumor MC distribution, investigating the pattern of distribution of tryptase-positive MCs around the blood vessels in human endometrial carcinoma samples by introducing a quantitative approach to characterize their spatial distribution.

Materials and methods

Immunohistochemistry

Paraffin-embedded tissue representatives of endometrial cancer grade III, endometrial cancer grade I, and non-neoplastic endometrium cases were sectioned at 3 μm. The sections were transferred onto poly-L-lysine-coated slides and subjected to deparaffinization and rehydratation. A double immunohistochemistry reaction was performed using the Envision commercial (Dako, Agilent Technologies, Santa Clara, CA, USA). Briefly, after standard heat antigen retrieval performed with a citrate buffer solution (Dako, Agilent Technologies, Santa Clara, CA, USA), endogenous peroxidases and alkaline phosphatases were blocked with a dual endogenous block solution. The samples were then incubated overnight at 4 °C with the first primary antibody against tryptase (Novocastra, Leica Biosystems, Nussloch, Germany) diluted 1:200 and visualized with a polymer/HRP secondary antibody using DAB as the first chromogen. Subsequently, samples were incubated for 30 min at room temperature with the second primary antibody against FVIII diluted 1:250 (Dako, Agilent Technologies, Santa Clara, CA, USA) and visualized with a polymer/AP secondary antibody using Fast Red as the second chromogen. Counterstaining was performed with Harris hematoxylin. Each immunohistochemistry reaction was coupled with a negative control reaction (no primary antibody).

Slide scanning and analysis

For each case, slides double stained for tryptase and FVIII were scanned using the whole-slide scanning platform Aperio ScanScope CS (Leica Biosystems, Nussloch, Germany). All the slides were scanned at the maximum magnification available (40×) and stored as digital high-resolution images on the workstation associated with the instrument.

Digital slides were inspected with the Aperio ImageScope v.11 software (Leica Biosystems, Nussloch, Germany) at 20× magnification. Tryptase-positive cells were counted in three high-power fields of equal area (40× magnification in the Aperio ScanScope system).

Distances between MCs and blood vessels and between MCs were assessed with the ruler tool in the Aperio ImageScope software using the center of the mast cell as the starting point of the measure and the center of the vessel lumen or the center of another mast cell as the end point of the measure. For the measurement purposes, only vessels with a recognizable shape and lumen were considered for the analysis (Fig. 1).

Image analysis methods

Computer-assisted image analysis was performed to characterize the distribution of MCs around the vessel profiles. The image analysis was performed by means of the scanning platform Aperio ScanScope CS (Leica). At a primary magnification of 20×, five randomly chosen fields per section were selected and their images acquired in full colors (RGB, 24-bit), processed to correct shading, and then filed TIFF. All the image analysis procedures were performed by using the ImageJ software, freely available at http://rsb.info.nih.gov/ij/.

The main steps of the image analysis procedure are illustrated in Fig. 2. Color deconvolution was first applied
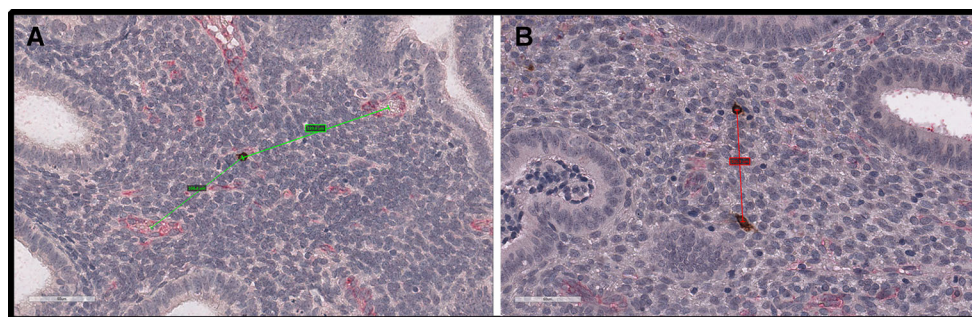
Fig. 1 Example of distance measurement. Distances were assessed with the ruler tool available in the ImageScope software. **a** Example of measurement of distance between a mast cell and blood vessels. **b** Example of measurement of distance between MCs
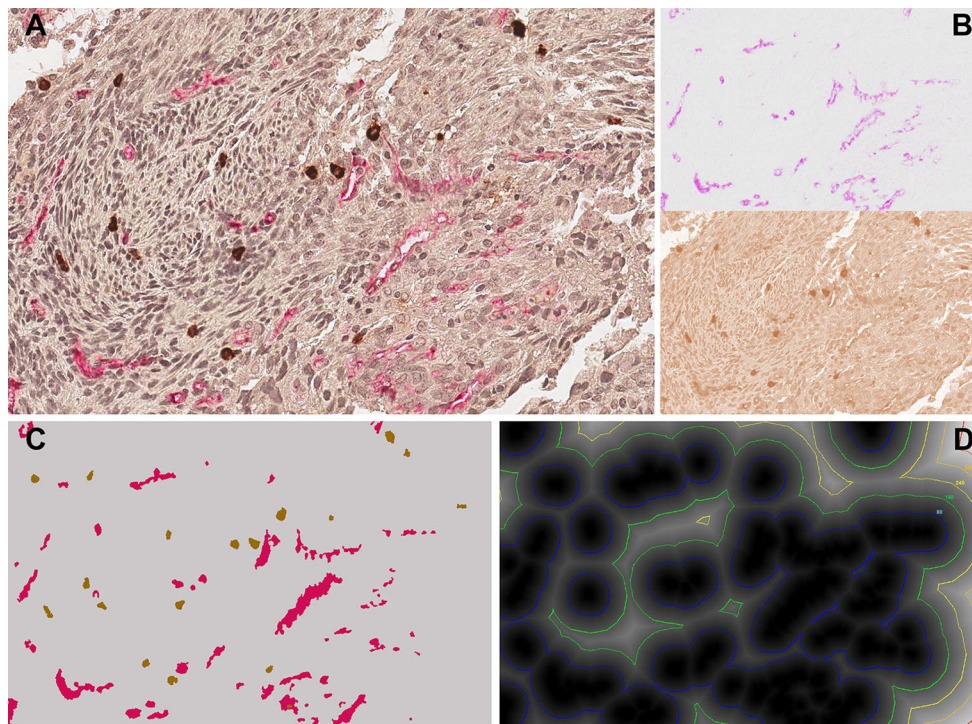
Fig. 2 Main steps of the image analysis procedure. **a** Field image analysis with CD31-positive vessels (*red*) and tryptase-positive MCs (*brown*). **b** By applying a color deconvolution procedure (see text), the two stains can be efficiently separated. **c** Binary image of the vessel profiles and MCs obtained by conventional thresholding of the images in B. **d** Distance transform of the image shown in **c**; background pixels are labeled according to their distance from the nearest vessel profile boundary as indicated by the *colored contour lines*. The distance of each cell profile from the vessels can be estimated by the value of the map at the point where the cell profile is located (i.e., at its *x*-, *y*-coordinates) (color figure online)

to allow the identification of vessels and MC profiles. This procedure implements stain separation according to the method by Ruifrok and Johnston [4] and was performed by using an ImageJ plug-in specifically developed by Gabriel Landini (see http://www.mecourse.com/landinig/software/software.html). As shown in Fig. 2b, this procedure allows the generation of two images containing CD31- and DAB-stained structures, respectively. From these images, vessel and MC profiles can then be easily discriminated by conventional thresholding methods (Fig. 2c) and the number and positions (i.e., *x*-, *y*-coordinates of the gravity centers) of MC profiles can be evaluated. To estimate the distance of each MC profile from the vessels, the binary image of the vessel profiles was further processed to calculate its "distance transform" [5]. This algorithm provides a map where each background pixel is labeled (Fig. 2d) with a value equal to its distance from the nearest pixel belonging to a vessel profile. The distance from vessels of each MC profile was then evaluated by the value the map exhibited at the location corresponding to the *x*-, *y*-coordinates of the cell profile. Around the observed set of vessel profiles, 50 random (Poisson) point patterns were finally computer generated. Each pattern had a number of points equal to the number of observed mast cell profiles. They underwent the previously described analysis in order to provide Monte Carlo estimates [6] of the distances from vessels in the case of complete spatial randomness (CSR).

Statistics

Within each sample, MC density values (number of cells per unit area of sampled tissue) and distances from the nearest vessel profile were averaged to provide a representative value for that sample. Differences between the groups of samples were then statistically tested by one-way analysis of variance followed by Bonferroni's test for multiple comparisons. The GraphPad Prism 3.0 statistical package (GraphPad Software Inc., San Diego CA, USA) was used for the analysis, and $p \leq 0.05$ was considered as the limit for statistical significance.

For each group, the cumulative frequency distribution [$G(d)$] of all the observed cell-to-vessel distances was calculated. Its expected value under CSR [$G_0(d)$] was estimated by averaging the cumulative frequency distributions of the distances from vessels obtained from the 50 simulated random point patterns. To interpret the cell-to-vessel spatial relationship statistically, the 95 % confidence envelope for $G_0(d)$ was also calculated from the Monte

Fig. 3 Mast cell counts progressively increase from non-neoplastic to grade III endometrial carcinoma. Representative images from **a** non-neoplastic endometrium, **b** grade I endometrial carcinoma, **c** grade III endometrial carcinoma. **d** Significant difference between the experimental groups in mast cell counts. $**p < 0.01$; $***p < 0.0001$
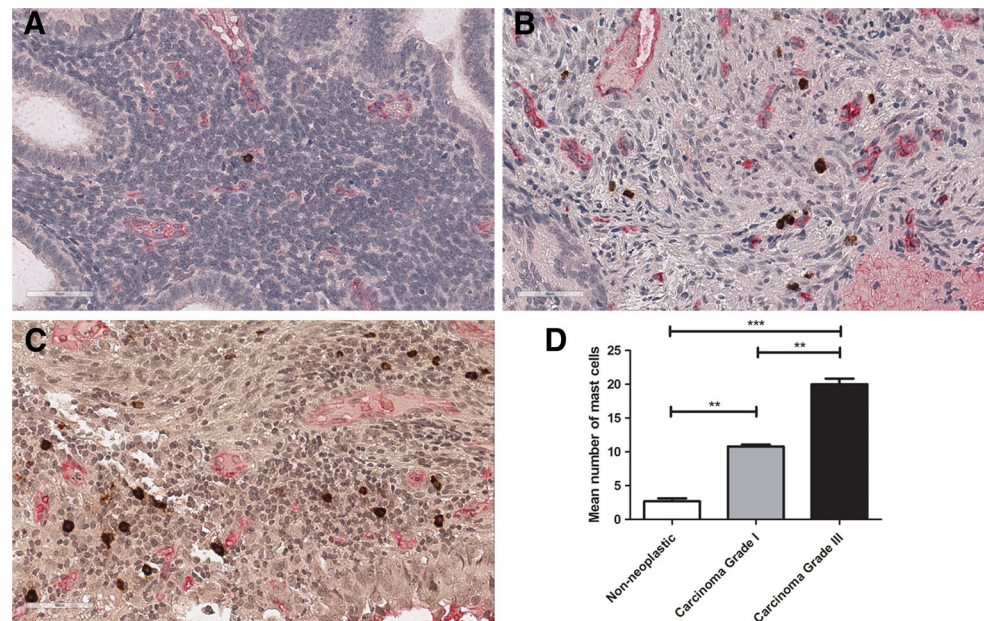
Carlo simulations [7]. The null hypothesis is that there is no difference between the two functions, i.e., $G(d) = G_0(d)$ for all d. Thus, if $G(d)$ is greater than the confidence envelope around $G_0(d)$, then the cells are clustered around the vessels, i.e., they are closer to the vessels than expected by chance. If $G(d)$ is lower than the envelope around $G_0(d)$, then short cell-to-vessel distances are less frequent than expected by chance; i.e., the placement of the cells close to the vessels was "inhibited" [8].

Results

Mast cell counts

Cell counting showed a significant difference ($p < 0.001$) in mean MCs number among the groups examined (Fig. 3). In particular, a progressively increased number of MCs was found with the lowest number of MCs detected in non-neoplastic endometrium (mean = 2.7 SD = 0.42), followed by an higher number of MCs in endometrial cancer grade I (mean = 10.80 SD = 0.28) and by the highest number detected in endometrial carcinoma grade III (mean = 20.00 SD = 0.85).

Distances between MCs and blood vessels

Measurements showed a significant difference in the mean distance between MCs and blood vessels among the groups (Fig. 4). Specifically, the mean distance in micrometers of MCs from vessels was significantly higher in the non-neoplastic endometrium (mean = 97.48 SD = 19.35)

when compared with grade I (mean = 40.63 SD = 5.85) and grade III (mean = 34.25 SD = 1.41) endometrial carcinoma indicating a closer spatial relationship between MCs and vessels in endometrial carcinoma. No significant difference was present in the mean distance of MCs from vessels between grade I and grade III endometrial carcinoma. Furthermore, distances between different MCs were not significantly different among the groups considered (Fig. 4).
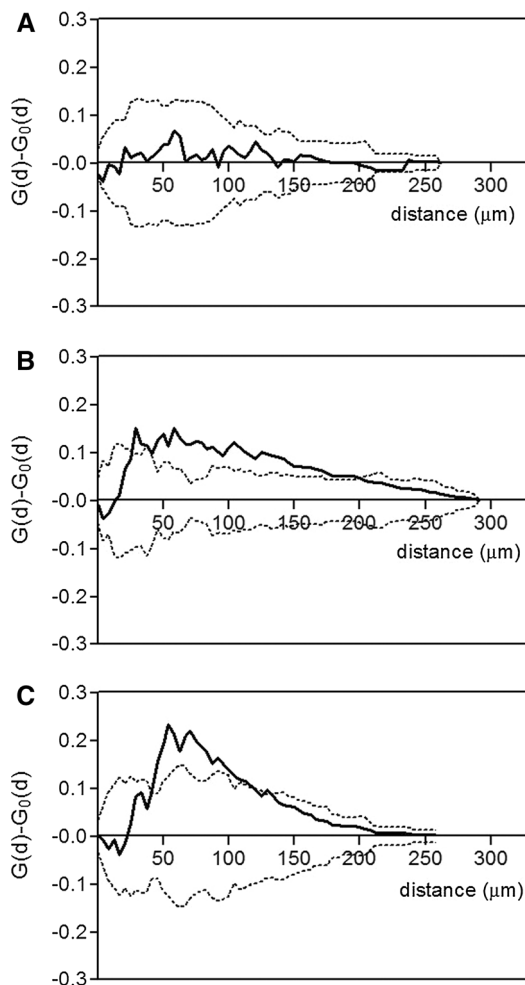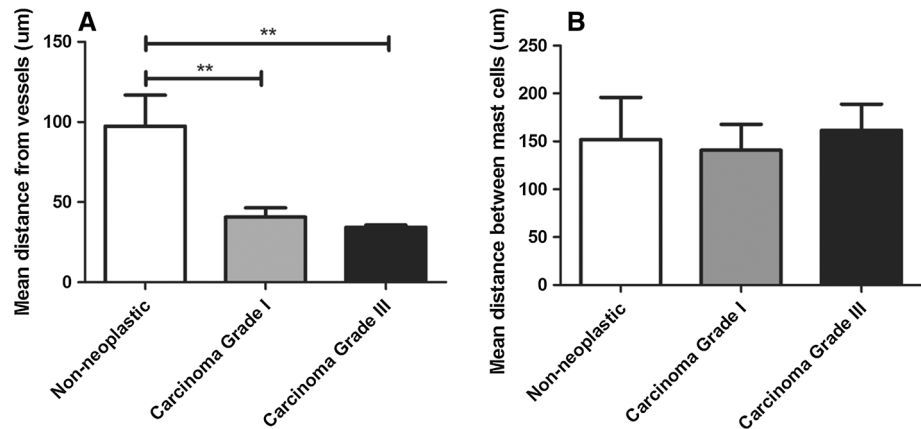
Analysis of the spatial relationship between MCs and microvessels

While in the control group, the spatial distribution of MCs was consistent with a random distribution (Fig. 5a), in both grade 1 and grade 3 groups it showed significant deviations from randomness. In particular, the cell pattern in both cases was clumped around the vessel profiles as indicated by a $G(d)$ significantly higher than expected under complete spatial randomness (Fig. 5b, c), suggesting a significant spatial association between MCs and vessels. Consistently, when compared to the control group, in both grade 1 and grade 3 groups the mean distance of MCs from vessels (Fig. 4) appeared significantly ($p < 0.01$) lower.

Discussion

MCs are widely distributed in connective tissue, and evidence has been provided of a mutual spatial and functional relationship between MCs and endothelial cells, since in many organs and under physiological conditions MCs are

Fig. 4 Distance measurements between MCs and vessels and between MCs. **a** Significant difference between non-neoplastic endometrium and carcinoma grades I and III in mean distance from blood vessels. **b** No significant difference among the experimental groups in mean distance between different MCs. **p** < 0.01

Fig. 5 Analysis of the spatial relationship between MCs and microvessels. *Solid lines* indicate the difference between the observed distribution of cell-to-vessel distances [$G(d)$] and the estimated distribution [$G_0(d)$] under complete spatial randomness (CSR). *Dotted lines* indicate the 95 % confidence envelope for CSR. While in the control group the spatial distribution of MCs was consistent with a random one (**a**), in both grade 1 (**b**) and grade 3 (**c**) groups there was a significant spatial association between MCs and vessels as indicated by a frequency of short cell-to-vessel distances significantly higher than expected by chance

localized close to capillaries and lymphatic channels [9–11]. Several lines of evidence have implicated MCs in the regulation of physiological or pathological examples of angiogenesis, including wound healing [12], ovulation [13], chronic inflammation [14], and tumor growth [15].

An increased number of MCs have been demonstrated in angiogenesis associated with vascular tumors, like hemangioma and hemangioblastoma [16, 17], as well as a number of hematological and solid tumors, including lymphomas [18–21], multiple myeloma [22], myelodysplastic syndrome [23], B cell chronic lymphocytic leukemia [24], breast cancer [25, 26], colon-rectal cancer [27], uterine and cervix cancer [1, 28, 29], melanoma [30–34], and pulmonary adenocarcinoma [35], in which mast cell accumulation correlates with increased neovascularization, mast cell vascular endothelial growth factor (VEGF) and fibroblast growth factor-2 (FGF-2) expression, tumor aggressiveness, and poor prognosis [33, 36].

A quantitative assessment of the spatial co-localization of MCs and vessels in tissue sections from the lesions of patients with primary melanoma as compared with samples from common acquired nevi was also provided [37]. In the present study, we have further expanded this quantitative approach to analyze the changes exhibited by the spatial distribution of MCs around the vessels in human endometrial cancer bioptic specimens as compared to normal tissue samples.

The approach here followed derived from spatial statistics [38, 39] and was based on the statistical analysis of the distribution of the distances of MCs from vessels with the aim to objectively establish whether the two structures (MCs and vessels) were distributed independently over the studied area or displayed any kind of spatial association. Such an analysis involved the comparison of the observed distribution of MC-to-vessel distances with the one corresponding to the case of complete spatial randomness, i.e., in which the MCs are distributed randomly over the studied area. To derive this reference

distribution, a simulation technique was applied [6], involving the computer generation of point patterns of the same size as the observed cell pattern, but placed in the area under investigation according to a random (Poisson) distribution [37].

The results of this study have shown that in human endometrial cancer bioptic specimens the spatial distribution of MCs shows significant deviation from randomness as compared with control group in which, instead, the spatial distribution of MCs is consistent with a random distribution. Shorter cell-to-vessel distances could be a morphological condition important to the increases in the rate of signal exchange among the cells and vessels [40, 41] and to the induction of higher concentrations of signaling molecules in the peri-cellular and peri-endothelial environment.

Overall, these findings confirm that MCs enhance tumor angiogenesis and their preferential localization along blood vessels and sites of new vessel formation sustaining the suggestion for an association between MCs and angiogenesis. However, the spatial association between vessels and MCs might simply reflect migrating MCs from the blood stream at vessel growing sites [42] indicating that these cells are involved in the maintenance reaction necessary for the long-lasting functional integrity of the endothelium [43].

Compliance with ethical standards

Conflict of interest The authors declare that they have no conflict of interest.

References

1. Ribatti D, Finato N, Crivellato E, Marzullo A, Mangieri D, Nico B, et al. Neovascularization and mast cells with tryptase activity increase simultaneously with pathologic progression in human endometrial cancer. Am J Obstet Gynecol. 2005;193(6):1961–5. doi:10.1016/j.ajog.2005.04.055.

2. Ribatti D, Nico B, Finato N, Crivellato E. Tryptase-positive mast cells and CD8-positive T cells in human endometrial cancer. Pathol Int. 2011;61(7):442–4. doi:10.1111/j.1440-1827.2011.02680.x.

3. Guidolin D, Nico B, Crivellato E, Marzullo A, Vacca A, Ribatti D. Tumoral mast cells exhibit a common spatial distribution. Cancer Lett. 2009;273(1):80–5. doi:10.1016/j.canlet.2008.07.032.

4. Ruifrok AC, Katz RL, Johnston DA. Comparison of quantification of histochemical staining by hue-saturation-intensity (HSI) transformation and color-deconvolution. Appl Immunohistochem Mol Morphol. 2003;11(1):85–91. doi:10.1097/00129039-200303000-00014.

5. Jc R. The image processing handbook. Boca Raton: CRC Press; 1995. p. 272.

6. Besag J, Diggle PJ. Simple monte carlo tests for spatial pattern. Appl Stat. 1977;26(3):327. doi:10.2307/2346974.

7. Gatrell AC, Bailey TC, Diggle PJ, Rowlingson BS. Spatial point pattern analysis and its application in geographical epidemiology. Trans Inst Br Geogr. 1996;21(1):256. doi:10.2307/622936.

8. Philimonenko AA, Janáček J, Hozák P. Statistical evaluation of colocalization patterns in immunogold labeling experiments. J Struct Biol. 2000;132(3):201–10. doi:10.1006/jsbi.2000.4326.

9. Eady RAJ, Cowen T, Marshall TF, Plummer V, Greaves MW. Mast cell population density, blood vessel density and histamine content in normal human skin. Br J Dermatol. 1979;100(6):623–33. doi:10.1111/j.1365-2133.1979.tb08065.x.

10. Rakusan K, Sarkar K, Turek Z, Wicker P. Mast cells in the rat heart during normal growth and in cardiac hypertrophy. Circ Res. 1990;66(2):511–6. doi:10.1161/01.res.66.2.511.

11. Rhodin JA, Fujita H. Capillary growth in the mesentery of normal young rats. Intravital video and electron microscope analyses. J Submicrosc Cytol Pathol. 1989;21(1):1–34.

12. Trabucchi E, Radaelli E, Marazzi M, Foschi D, Musazzi M, Veronesi AM, et al. The role of mast cells in wound healing. Int J Tissue React. 1988;10(6):367–72.

13. Krishna A, Beesley K, Terranova PF. Histamine, mast cells and ovarian function. J Endocrinol. 1989;120(3):363–71. doi:10.1677/joe.0.1200363.

14. Yamada T, Sawatsubashi M, Itoh Y, Edakuni G, Mori M, Robert L, et al. Localization of vascular endothelial growth factor in synovial membrane mast cells: examination with "multi-labelling subtraction immunostaining". Virchows Arch. 1998;433(6):567–70. doi:10.1007/s004280050290.

15. Ribatti D. Mast cells and macrophages exert beneficial and detrimental effects on tumor progression and angiogenesis. Immunol Lett. 2013;152(2):83–8. doi:10.1016/j.imlet.2013.05.003.

16. Glowacki J, Mulliken JB. Mast cells in hemangiomas and vascular malformations. Pediatrics. 1982;70(1):48–51.

17. Qu Z, Kayton RJ, Ahmadi P, Liebler JM, Powers MR, Planck SR, et al. Ultrastructural immunolocalization of basic fibroblast growth factor in mast cell secretory granules: morphological evidence for bFGF release through degranulation. J Histochem Cytochem. 1998;46(10):1119–28. doi:10.1177/002215549804601004.

18. Fukushima N, Satoh T, Sano M, Tokunaga O. Angiogenesis and mast cells in non-Hodgkin's lymphoma: a strong correlation in angioimmunoblastic T-cell lymphoma. Leuk Lymphoma. 2001;42(4):709–20. doi:10.3109/10428190109099333.

19. Marinaccio C, Ingravallo G, Gaudio F, Perrone T, Nico B, Maoirano E, et al. Microvascular density, CD68 and tryptase expression in human diffuse large B-cell lymphoma. Leuk Res. 2014;38(11):1374–7. doi:10.1016/j.leukres.2014.09.007.

20. Ribatti D, Nico B, Vacca A, Marzullo A, Calvi N, Roncali L, et al. Do mast cells help to induce angiogenesis in B-cell non-Hodgkin's lymphomas? Br J Cancer. 1998;77(11):1900–6. doi:10.1038/bjc.1998.316.

21. Ribatti D, Vacca A, Marzullo A, Nico B, Ria R, Roncali L, et al. Angiogenesis and mast cell density with tryptase activity increase simultaneously with pathological progression in B-cell non-Hodgkin's lymphomas. Int J Cancer. 2000;85(2):171–5. doi:10.1002/(sici)1097-0215(20000115)85:2<171:aid-ijc4>3.0.co;2-w.

22. Ribatti D, Vacca A, Nico B, Quondamatteo F, Ria R, Minischetti M, et al. Bone marrow angiogenesis and mast cell density increase simultaneously with progression of human multiple myeloma. Br J Cancer. 1999;79(3/4):451–5. doi:10.1038/sj.bjc.6690070.

23. Ribatti D, Polimeno G, Vacca A, Marzullo A, Crivellato E, Nico B, et al. Correlation of bone marrow angiogenesis and mast cells

with tryptase activity in myelodysplastic syndromes. Leukemia. 2002;16(9):1680–4. doi:10.1038/sj.leu.2402586.

24. Molica S, Vacca A, Crivellato E, Cuneo A, Ribatti D. Tryptase-positive mast cells predict clinical outcome of patients with early B-cell chronic lymphocytic leukemia. Eur J Haematol. 2003;71(2):137–9. doi:10.1034/j.1600-0609.2003.00110.x.

25. Bowrey PF, King J, Magarey C, Schwartz P, Marr P, Bolton E, et al. Histamine, mast cells and tumour cell proliferation in breast cancer: does preoperative cimetidine administration have an effect? Br J Cancer. 2000;82(1):167–70. doi:10.1054/bjoc.1999.0895.

26. Hartveit F. Mast cells and metachromasia in human breast cancer: their occurrence, significance and consequence: a preliminary report. J Pathol. 1981;134(1):7–11. doi:10.1002/path.1711340103.

27. Lachter J, Stein M, Lichtig C, Eidelman S, Munichor M. Mast cells in colorectal neoplasias and premalignant disorders. Dis Colon Rectum. 1995;38(3):290–3. doi:10.1007/bf02055605.

28. Benitez-Bribiesca L, Wong A, Utrera D, Castellanos E. The role of mast cell tryptase in neoangiogenesis of premalignant and malignant lesions of the uterine cervix. J Histochem Cytochem. 2001;49(8):1061–2. doi:10.1177/002215540104900816.

29. Graham RM, Graham JB. Mast cells and cancer of the cervix. Surg Gynecol Obstet. 1966;123(1):3–9.

30. Dvorak AM, Mihm MC Jr, Osage JE, Dvorak HF. Melanoma. An ultrastructural study of the host inflammatory and vascular responses. J Investig Dermatol. 1980;75(5):388–93. doi:10.1111/1523-1747.ep12523627.

31. Reed JA, McNutt NS, Bogdany JK, Albino AP. Expression of the mast cell growth factor interleukin-3 in melanocytic lesions correlates with an increased number of mast cells in the perilesional stroma: implications for melanoma progression. J Cutan Pathol. 1996;23(6):495–505. doi:10.1111/j.1600-0560.1996.tb01441.x.

32. Ribatti D, Ennas MG, Vacca A, Ferreli F, Nico B, Orru S, et al. Tumor vascularity and tryptase-positive mast cells correlate with a poor prognosis in melanoma. Eur J Clin Investig. 2003;33(5):420–5. doi:10.1046/j.1365-2362.2003.01152.x.

33. Ribatti D, Molica S, Vacca A, Nico B, Crivellato E, Roccaro AM, et al. Tryptase-positive mast cells correlate positively with bone marrow angiogenesis in B-cell chronic lymphocytic leukemia. Leukemia. 2003;17(7):1428–30. doi:10.1038/sj.leu.2402970.

34. Ribatti D, Vacca A, Ria R, Marzullo A, Nico B, Filotico R, et al. Neovascularisation, expression of fibroblast growth factor-2, and mast cells with tryptase activity increase simultaneously with pathological progression in human malignant melanoma. Eur J Cancer. 2003;39(5):666–74. doi:10.1016/s0959-8049(02)00150-8.

35. Ullah E, Nagi A, Lail R. Angiogenesis and mast cell density in invasive pulmonary adenocarcinoma. J Can Res Ther. 2012;8(4):537. doi:10.4103/0973-1482.106530.

36. Toth-Jakatics R, Jimi S, Takebayashi S, Kawamoto N. Cutaneous malignant melanoma: correlation between neovascularization and peritumor accumulation of mast cells overexpressing vascular endothelial growth factor. Hum Pathol. 2000;31(8):955–60.

37. Guidolin D, Crivellato E, Nico B, Andreis P, Nussdorfer G, Ribatti D. An image analysis of the spatial distribution of perivascular mast cells in human melanoma. Int J Mol Med. 2006;. doi:10.3892/ijmm.17.6.981.

38. Bd R. Tests for randomness for spatial point patterns. J R Stat Soc. 1979;B41:368–74.

39. Pj D. Statistical analysis of spatial point patterns. London: Academic Press; 1983. p. 354.

40. Meininger CJ. Mast cells and tumor-associated angiogenesis. Chem Immunol. 1995;62:239–57.

41. Mierke CT, Ballmaier M, Manns MP, Welte K, Bischoff SC. Endothelial cells support survival of human intestinal mast cells by a direct cell-cell interaction. Gastroenterology. 2000;118(4):A360–1. doi:10.1016/s0016-5085(00)83547-7.

42. Silverman AJ, Sutherland AK, Wilhelm M, Silver R. Mast cells migrate from blood to brain. J Neurosci. 2000;20(1):401–8.

43. Watanabe Y, Lee SW, Detmar M, Ajioka I, Dvorak HF. Vascular permeability factor/vascular endothelial growth factor (VPF/VEGF) delays and induces escape from senescence in human dermal microvascular endothelial cells. Oncogene. 1997;14(17):2025–32. doi:10.1038/sj.onc.1201033.